Reactive Transport Parameter Estimation: Genetic Algorithm vs. Monte Carlo Approach

Samer Majdalani, Marwan Fahs, Jérôme Carrayrou, and Philippe Ackerer
Laboratoire d'Hydrologie et de Géochimie de Strasbourg, Université de Strasbourg/CNRS, Ecole et Observatoire des Sciences de la Terre, 1 rue Blessig, 67084 Strasbourg, France

DOI 10.1002/aic.11796
Published online June 22, 2009 in Wiley InterScience (www.interscience.wiley.com).

This article concerns reactive transport in porous media with an emphasis on the optimization of the chemical parameters. The transport of Cadmium (Cd) and tributyltin (TBT) in column experiments were used as test cases. The reactive transport model is described by a set of chemical reactions with equilibrium constants as the main adjustable parameters. As such a problem is highly nonlinear and can have multiple minima, global parameter estimation methods are more suitable than local gradient-based methods. This article focuses on the application of a genetic algorithm (GA) in estimating chemical equilibrium parameters of a reactive transport model. The GA is capable of minimizing the difference between the measured and modeled breakthrough curves for both Cd and TBT. A comparison between GA and Monte-Carlo approaches shows that the GA performance is better than the Monte-Carlo, especially for a small number of evaluations of the cost function. The results of this study show that the use of GA to estimate the parameters of reactive transport models is promising. © 2009 American Institute of Chemical Engineers *AIChE J,* 55: 1959–1968, 2009
Keywords: reactive transport, chemical equilibrium constants, surface complexation modeling, parameter estimation, genetic algorithm, Monte-Carlo

Introduction

Reactive transport models are increasingly used to improve understanding and provide prevision in hydrogeology and geochemistry fields.[1–5] In this article, we address the modeling of both Cadmium (Cd) and tributyltin (TBT) transport in column experiments. Cd is a potentially toxic heavy metal. Anthropogenic activities, such as industrial waste disposal and fertilizer application on land, have led to the accumulation of Cd in the environment and its entry into the food chain.[6] TBT is a highly toxic compound, which has been produced on a large scale to be used in ship antifouling paints, preservation of wood, and disinfection of circulating industrial cooling waters. Because of its widespread use as an antifouling agent in boat paints, TBT has been introduced into aquatic ecosystems.[7]

Correspondence concerning this article should be addressed to S. Majdalani at samer.majdalani@imfs.u-strasbg.fr.

In this study, the sorption of Cd and TBT onto natural quartz sand is described by the diffuse layer model (DLM).[8] Besides the hydraulic properties of the domain, our reactive transport model is described by a set of chemical reactions with corresponding equilibrium constants as adjustable parameters. Usually, the estimation of the required chemical parameters is done either by trial and error or with tools, such as FITEQL,[9] MINTEQA2,[10] GRFIT,[11] and CXTFIT2.0,[12] which use local gradient-based methods. In a previous study, Aggarwal and Carrayrou[13] showed that the parameters space of such a problem can have multiple local minima. Therefore, global inverse methods could be more suitable than local ones in estimating equilibrium chemical parameters.

For nonlinear problems, such as equilibrium chemical equations, the efficiency of local methods decreases strongly.[14,15] Even though the mathematical formalism of our problem is quite straightforward, the nonlinearity of sorption associated with multi-species transport yields cumbersome calculations. In addition, the problem is reputed to

be weakly convex, which makes it very difficult to seek parameters by means of classical techniques, which are usually based on descent methods assuming that model sensitivities to parameters are affordable. For rapid convergence, second-order derivatives of the state variable with respect to parameters (the so-called Hessian matrix) should also be computed or approximated. It is obvious that the nonlinearity of the sorption reactions does not help to get these features and that the analytical derivations of concentrations (state variables) with respect to parameters are hard to obtain. It is also quite certain that a perturbation technique for these derivations would yield poor results. Therefore, the use of alternative methods that do not necessitate analytical derivations of concentrations with respect to parameters is better suited for our problem.

Genetic algorithms (GAs) are a class of global stochastic search methods based on concepts of genetic recombination and natural selection.[16,17] Because of their robustness and general applicability, GAs have been used in the optimization of nonlinear problems in various fields including estimation of preferential water flow parameters in natural soil columns,[18] optimization of semibatch reactive crystallization processes,[19] optimal configuration of batch distillation,[20] and global optimization of a dryer.[21] The aforementioned studies are only a few examples, and readers interested in the basics of GAs can refer to the review by Goldberg.[22]

Today, there is an increasing interest in using global methods to estimate parameters of reactive transport models. For example, GAs were recently used for the estimation of *kinetic* parameters in reactive transport models.[23,24] For the estimation of chemical *equilibrium* parameters in reactive transport models, the only global method reported in literature (to our knowledge) is the Monte-Carlo approach.[13] This article introduces a first application of GA to estimate chemical *equilibrium* parameters in reactive transport models. It also aims to compare the performances of both GA and Monte-Carlo approaches. After a brief description of the reactive transport model and the GA and the Monte-Carlo approaches, we show the GA optimization results and discuss the efficiency of the parameter estimation methods used in this study.

Reactive Transport and Diffuse Layer Model

Column experiments evaluating the sorption of Cd on Cristobalite and TBT on natural quartz sand were used as test cases. More details about the experimental setup and Cd (respectively TBT) breakthrough curves can be found in Bürgisser[25] (respectively Bueno et al.[26]). For these cases, the chemical system is formed by N_c aqueous and sorbed species $[C_{i\ (i=1,\ N_c)}]$. Under the assumption of an instantaneous equilibrium, the chemical system can be simplified using the definitions of components and species. Among the species, we select N_x components $[X_{j\ (j=1,\ N_x)}]$, which are a set of linearly independent chemical entities such that every chemical species can be uniquely represented as a linear combination of these components.

The chemical system is described by mass action and conservation laws. The mass action laws (1) are written for the formation of the N_c species C_i by the selected component set X_j:

$$[C_i] = K_i \prod_{j=1}^{N_x} [X_j]^{a_{i,j}} \qquad \text{for } i = 1 \text{ to } N_c, \tag{1}$$

where the concentration of species and components is noted [–], K_i is the equilibrium constant, and $a_{i,j}$ are the stoichiometric coefficients for the chemical reactions. The conservation law (2) is written to preserve the total quantity $[T_j]$ (mol m^{-3}) of each component:

$$[T_j] = [Td_j] + [Tf_j] = \sum_{i=1}^{N_c} a_{i,j}[C_i] \qquad \text{for } j = 1 \text{ to } N_x, \tag{2}$$

where $[Td_j]$ (mol m^{-3}) is the total mobile concentration of component j and $[Tf_j]$ (mol m^{-3}) is the total fixed concentration of component j.

The transport phenomenon is governed by the advection-dispersion-reaction (ADR) equation for the components:

$$\omega \frac{\partial [T_j]}{\partial t} = \nabla \cdot (D \cdot \nabla [Td_j]) - U \cdot \nabla [Td_j] \qquad \text{for } j = 1 \text{ to } N_x, \tag{3}$$

where ω [–] is the effective porosity, D (m^2 s^{-1}) is the dispersion/diffusion tensor, and U (m s^{-1}) is the Darcy velocity.

Sorption phenomena can be described by ion exchange or by surface complexation. For ion exchange, the mass action law describing the formation of a species is given in Eq. 1. For the surface complexation phenomenon, the sorption site should be defined as a component *XS*. Then the potential of the surface ψ is added to the mass action law describing the sorption of a species Cs_i:

$$[Cs_i] = K_i \exp\left(-\frac{z_i f}{R\tau}\psi\right) \prod_{j=1}^{N_x} [X_j]^{a_{i,j}}, \tag{4}$$

where z_i is the charge of the species Cs_i, R (J mol^{-1} K^{-1}) is the gas constant, f (C mol^{-1}) is the Faraday constant, and τ (K) is the Kelvin temperature. Different models can be used to obtain the potential ψ from the electrostatic charge fixed at the surface. The major idea of these models is that the sorption of an electrically charged species onto a surface will modify the electrical charge of this surface. A potential is then created that helps the sorption of species of opposite charge or impedes the sorption of species of the same charge.

To describe the relationship between the charge of the surface and the potential, we use the DLM. In the DLM, the potential decreases exponentially with the distance to the surface:

$$\sum_{\text{sorbed}} z_i [Cs_i] = \frac{SM}{f} (8R\tau\varepsilon\varepsilon_0 I)^{1/2} \sinh\left[\frac{Z_{el} f \psi}{2R\tau}\right], \tag{5}$$

where S (m^2 kg^{-1}) is the specific area of the solid, M (kg m^{-3}) the mass concentration of the solid, ε_0 (F m^{-1}) the permittivity of the vacuum, ε (F m^{-1}) the permittivity of the water, Z_{el} the electrical charge of counter-ion, and I (mol m^{-3}) the ionic strength.

Hydrodynamic parameters such as porosity, velocity, or dispersivity are estimated from a tracer experiment. In the same way, chemical parameters for aqueous reactions, such

Table 1. Morel Tableau for the Cd Reactive Transport Test Case

		Aqueous Components						Adsorbed Component		
		H^+	Cl^-	NO_3^-	Na^+	Im	TBT^+	$\equiv$S—OH	Ψ_S	log (K)
Aqueous species	OH^-	−1								−14.0
	ImH^+	1				1				7.0
	$ImTBT^+$					1	1			3.91
	TBTOH	−1					1			−6.25
	TBTCl		1				1			0.6
	$TBTNO_3$			1			1			0.62
Adsorbed species	$\equiv S—OH_2^+$	1						1	1	**6**
	$\equiv S—O^-$	−1						1	−1	**−2**
	$\equiv$S—OTBT	−1					1	1		**7.5**
	$\equiv S—OHTBT^+$						1	1	1	**9**
	$\equiv$S—ONa	−1			1			1		**−1**
	Initial condition (M)	Fixed	0.0	0.1	0.1	10^{-3}	0.0	$\mathbf{3.16 \times 10^{-6}}$		
	Injection (M)	Fixed	8.6×10^{-6}	0.1	0.1	10^{-3}	8.6×10^{-6}			
	Leaching (M)	Fixed	0.0	0.1	0.1	10^{-3}	0.0			

Bold parameters will be estimated.

as equilibrium constants and initial concentrations, are obtained from thermodynamic databases. During the transport, the aqueous components react with the solid ion exchange sites (S).

The direct problem is solved using the operator splitting (OS) approach,[27] in which transport and chemical equations are solved sequentially. In the transport equation, the advective term is discretized by the Galerkin Discontinuous Finite Element method, whereas the dispersive term is discretized by the Mixed Hybrid Finite Element method. The space discretization is done with a 1D regular mesh with 20 and 35 elements for TBT and Cd, respectively. The nonlinear chemical equations are solved by the Newton-Raphson method. The convergence of this method is verified by means of a maximum relative convergence criterion, $\left|\left(X_j^{m+1} - X_j^m\right) \middle/ X_j^{m+1}\right|_\infty < \varepsilon_{NR}$, where m represents the iteration and ε_{NR} is a user-defined small number (10^{-7} for our simulation).

In the case of sorption of TBT on natural quartz sand, five reactions of ion exchange occur between chemical species and the adsorbed component $\equiv$S—OH, leading to five adsorbed species ($\equiv S—OH_2^+$, $\equiv S—O^-$, $\equiv$S—OTBT, $\equiv S—OHTBT^+$, $\equiv$S—ONa). Chemical reactions, constants of equilibrium, initial and inflow boundary conditions for the TBT are summarized in Table 1 (in which the bold parameters are the ones to be estimated). Only chemical parameters related to the solid-water interface phenomena (i.e., sorption parameters) are estimated: equilibrium constants for sorption reactions ($K_{\equiv S—OH_2^+}$, $K_{\equiv S—O^-}$, $K_{\equiv S—OTBT}$, $K_{\equiv S—OHTBT^+}$, $K_{\equiv S—ONa}$) and initial total concentration for sorption components ($T_{\equiv S—OH}$).

In the case of sorption of Cd on Cristobalite, two types of reactions occur. By ion exchange, two adsorbed species $\equiv S_E—H$ and $\equiv(S_E)_2—Cd$ are formed from the component $\equiv S_E—Na$. Two reactions of surface complexation lead to the formation of $\equiv S_C—O^-$ and $\equiv S_C—OCdOH$ using the component $\equiv S_C—OH$. Chemical reactions, constants of equilibrium, initial and inflow boundary conditions for the Cd are summarized in Table 2 (where the bolt parameters are the ones to be estimated). Only sorption parameters are estimated: equilibrium constants for sorption reactions ($K_{\equiv S_C—O^-}$, $K_{\equiv S_C—OCdOH}$, $K_{\equiv S_E—H}$, $K_{\equiv(S_E)_2—Cd}$) and initial total concentration for sorption components ($T_{\equiv S_C—OH}$, $T_{\equiv S_E—Na}$).

For the two test cases, we focus on the estimation of parameters related to solid water reactions, and we assume that parameters related to reactions in water phase are well known. The total concentration in the water phase can either be obtained by analytical methods (ionic chromatography) or controlled during the experiment. The number of sorption sites for a given solid is very difficult to measure by analytical methods (XPS can give an estimation if the solid is powdered but is not adapted for grains). Equilibrium constants for water phase reactions are very well documented, whereas data bases containing equilibrium constants for solid-water reactions are not.

Binary GA Components

Parameters space

In this study, we used a binary GA[28] that uses a classical binary coding of parameters. The binary coding of parameters allows for the parameters to be defined as discrete values (opposed to continuous) within a prescribed range. The GA defines a chromosome as an array of parameter values to be optimized, where each chromosome is chosen from a finite parameters space consisting of discrete values. The binary encoding of each parameter value is called a gene (i.e., array of 0 and 1 bits), and thus, a chromosome is written as a series of several genes with a total of N_{bits}.

The binary coding differs from the so-called Gray code. In a Gray code, the gradual passage from a value to the following/preceding one is done by modifying only one bit, whereas in a binary code the same action requires the modification of two bits. The use of Gray code would have been adequate if we wanted to compare the GA with another method that gradually modifies the values of parameters (like local descent methods). In this study, we aimed to compare the GA with the Monte Carlo method in which values are randomly changed without taking into account their gradual variation. For this reason, we chose to use the binary coding.

Table 2. Morel Tableau for the TBT Reactive Transport Test Case

			Aqueous Components				Adsorbed Components			
			H^+	Na^+	NO	Cd^{2+}	$\equiv S_E$ —Na	$\equiv S_C$—OH	Ψ_S	log (K)
Aqueous species		H^+	1							0
		OH^-	−1							−13.91
		Na^+		1						0
		NO_3^-			1					0
		Cd^{2+}				1				0
		$CdOH^+$	−1			1				−10.17
		$Cd(OH)_2$	−2			1				−20.44
		$Cd(OH)_3^-$	−3			1				−33.3
		$Cd(OH)_4^{2-}$	−4			1				−47.17
		Cd_2OH^{3+}	−1			2				−9.3
		$Cd_4(OH)_4^{4+}$	−4			4				−32.67
		$CdNO_3^+$			1	1				0.46
		$Cd(NO_3)_2$			2	1				0.17
		$Cd(NO_3)_3^-$			3	1				−0.85
Adsorbed species	Surface complexation	$\equiv S_C$—OH						1		0
		$\equiv S_C$—O^-	−1					1	−1	**1**
		$\equiv S_C$—OCdOH	−2			1		1		**−8**
	Ion exchange	$\equiv S_E$—Na								0
		$\equiv S_E$—H	1	−1			1			**2**
		$\equiv (S_E)_2$—Cd		−2		1	2			**0.5**
		Initial condition (M)	1.2×10^5	10^{-2}	10^{-2}	0	$\mathbf{1.78 \times 10^{-4}}$	$\mathbf{5.62 \times 10^{-4}}$		
		Injection (M)	-10^{-5}	10^{-2}	10^{-2}	1.7×10^{-5}				
		Leaching (M)	1.2×10^5	10^{-2}	10^{-2}	0				

Bold parameters will be estimated.

In the TBT test case, we built the parameters space around values found in the literature[13,29,30] in the following manner: log ($K_{\equiv S-OH_2^+}$) varies between [−3; 12.5] with a step of 0.5, log ($K_{\equiv S-O^-}$) varies between [−10; 5] with a step of 1, log ($K_{\equiv S-OTBT}$) varies between [−3; 12.5] with a step of 0.5, log ($K_{\equiv S-OHTBT^+}$) varies between [−3; 12.5] with a step of 0.5, log ($K_{\equiv S-ONa}$) varies between [−7; 8] with a step of 1, and $T_{\equiv S-OH}$ varies between [10^{-9}; $10^{-1.5}$] with a step of $10^{0.5}$. The resulting parameters space consists of 134 217 728 sets of parameters.

For the Cd test case, the parameters space was also built around literature values[31–37]: log ($K_{\equiv S_C-O^-}$) varies between [−10; 5] with a step of 1, log ($K_{\equiv S_C-OCdOH}$) varies between [−14; −6.5] with a step of 0.5, log ($K_{\equiv S_E-H}$) varies between [−7; 8.5] with a step of 0.5, log ($K_{\equiv (S_E)_2-Cd}$) varies between [−7; 8.5] with a step of 0.5, $T_{\equiv S_C-OH}$ varies between [10^{-9}; $10^{-1.25}$] with a step of $10^{0.25}$, and $T_{\equiv S_E-Na}$ varies between [10^{-9}; $10^{-1.25}$] with a step of $10^{0.25}$. The resulting parameters space consists of 268 435 456 sets of parameters.

The choice of the steps was based on the parameter variation that can cause a change of the cost value to the order of 10^{-3}.

Cost function

The optimization is done by minimizing the error (i.e., cost function) between experimental and simulated values according to:

$$\text{cost} = \frac{1}{N_{\text{exp}}} \sum_{N_{\text{exp}}} \sqrt{\left(\frac{C_{\text{exp}} - C_{\text{sim}}}{C_{\text{exp}}}\right)^2}, \tag{6}$$

where N_{exp} is the number of experimental points, C_{exp} and C_{sim}, respectively, are the experimental and simulated dissolved concentrations of TBT or Cd at the column outlet.

Natural selection and pairing

The GA starts with an initial population of N_{pop} chromosomes ($N_{\text{pop}} = 8$ in this study), which is an $N_{\text{pop}} \times N_{\text{bits}}$ matrix filled with randomly generated one and zero bits. The chromosomes are then decoded to evaluate their costs, and ranked from the lowest to the highest cost. A portion of the high-cost chromosomes (50% of the population) are discarded through natural selection or survival of the fittest. Natural selection occurs each generation or iteration of the algorithm. Every iteration, half of the N_{pop} chromosomes (N_{good}) are placed in a mating pool for reproducing whereas the discarded chromosomes (N_{bad}) are replaced by new offspring.

Two chromosomes are selected from the mating pool of N_{good} chromosomes to produce two new offspring. Pairing takes place in the mating population until N_{bad} offspring are born to replace the discarded chromosomes and reconstitute the N_{pop} members of the population. Based on the recommendations of Majdalani et al.,[18] we used a pairing from the top-to-bottom technique. This technique starts at the top of the list and pairs the chromosomes two at a time until the top N_{good} chromosomes are selected for mating. Thus, the algorithm pairs chromosome$_{2i-1}$ with chromosome$_{2i}$ for $i = 1, 2$.

Mating and mutations

Mating is the creation of two offspring from the two parents selected in the pairing process. The technique used in this study is the single-point crossover in which a crossover point is randomly selected between the first and last bits of the parents' chromosomes. Mutations alter a small percentage of the bits in the list of chromosomes. A single point mutation changes a "1" to "0" or vice versa. Mutation points are randomly selected from the total number of

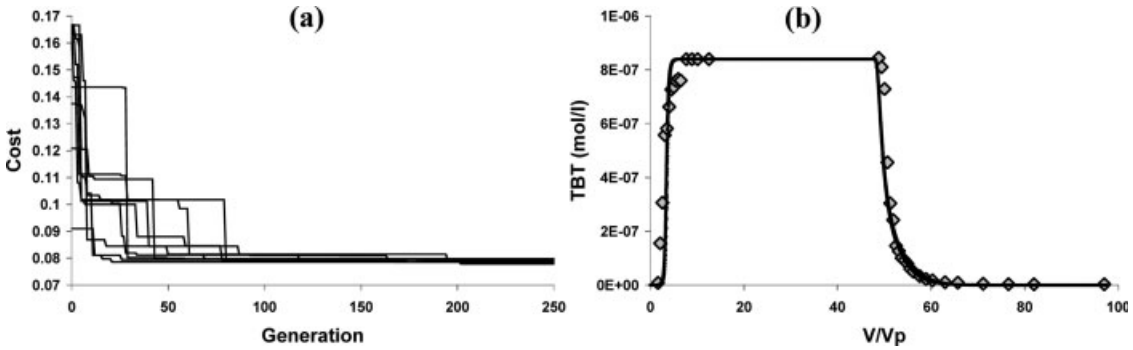

Figure 1. Estimating chemical equilibrium parameters for the TBT reactive transport test case using GA inverse method.

(a) Evolution of the cost function over 250 generations for 10 replicated runs. (b) Experimental breakthrough curve and its simulation with the optimized parameters for 10 replicated runs. ◇ shows experimental data; lines show simulations.

$N_{pop} \times N_{bits}$ bits in the population matrix. The number of mutations ($N_{mutations}$) is determined on the basis of a mutation rate, μ, ($0 < \mu < 1$) by $N_{mutations} = \mu \times N_{pop} \times N_{bits}$. Mutations do not occur on the final iteration. Also, mutations are not allowed on the best solutions, which are designated as elite solutions. Elitism consists of letting the best elements (N_{elite}) propagate unchanged. After the mutations, the costs associated with the offspring and mutated chromosomes are calculated and ranked. Thus, a new generation is obtained. In this study, we chose $\mu = 0.25$ and $N_{elite} = 1$, based on the recommendations of Majdalani et al.[18]

Convergence

The process described is run for several generations ($N_{generations}$). We wanted to limit the number of function evaluations by run (S) in the range of one per 10^5 of the parameters space (about 2×10^8 parameters sets), which gives $S = 2000$. Thus, if a total of S number of function evaluations are allocated, a GA with a population size of $N_{pop} = 8$ must be run for a maximum of[38]: $N_{generations} = S/N_{pop} = 250$.

Monte-Carlo Approach

The parameters **P**, which have to be estimated, are randomly generated. The distribution of each parameter P_i describes a Gaussian distribution. Each Gaussian distribution is set by its mean $\overline{P}_i$ and its standard deviation σ_i. The Latin Hyper Cube procedure (LHC, Hydranto, 2003) is used for sampling random numbers from a given set of probability distribution. In LHC, the given range of parameter values is divided into regions of equal probability. A random value of parameter is then generated in each interval. This method ensures the cover of the whole range of parameter values.

In each minimization step i, N_i sets of parameters are generated from the mean $\overline{\mathbf{P}}^i$ and the standard deviation $\boldsymbol{\sigma}^i$ (initial mean $\overline{\mathbf{P}}^0$ and standard deviation $\boldsymbol{\sigma}^0$ given by the modeler). The reactive transport problem is solved with these sets of parameters and the cost function $F(\mathbf{P}^k)$ is calculated for $k = 1$ to N_i. The smallest $F(\mathbf{P}^{Optimal})$ is then selected. In the following minimization step $i + 1$, the mean $\overline{\mathbf{P}}^{i+1}$ and standard deviation $\boldsymbol{\sigma}^{i+1}$ are modified by taking $\overline{\mathbf{P}}^{i+1} = \mathbf{P}^{Optimal}$ and $\boldsymbol{\sigma}^{i+1} = \text{Max}\ [|\mathbf{P}^{Optimal} - \overline{\mathbf{P}}^i|; (\alpha_\sigma\ \boldsymbol{\sigma}^i)]$ with $\alpha_\sigma = 0.5$. More details about the Monte-Carlo inverse method are found in Aggarwal and Carrayrou.[13]

Results and Discussion

The GA optimization results

TBT test case. As a first attempt to discover the domain of possible solutions (optimized sorption parameters), 10 runs were replicated for the TBT test case (Figure 1). The ensemble evolution of the cost as a function of the number of generations ($N_{generation}$) shows a sharp decrease of the cost for earlier generations followed by a very slight decrease for high $N_{generation}$ (Figure 1a). The differences between the 10 runs are a result of the stochastic features of the algorithm. These

Table 3. Optimized Values of Sorption Parameters for the TBT Test Case Using GAs for 10 Replicated Runs

	log (K)						
Run #	$\equiv$S$-$OH$_2^+$	$\equiv$S$-$O$^-$	$\equiv$S$-$OTBT	$\equiv$S$-$OHTBT$^+$	$\equiv$S$-$ONa	$T_{\equiv S-OH}$ (M)	Cost
1	6	−2	7.5	9	−1	3.16×10^{-6}	0.0785
2	5.5	−5	7	8	−1	3.16×10^{-6}	0.0792
3	4	−5	5.5	7.5	−2	3.16×10^{-6}	0.0792
4	1.5	3	9.5	10.5	2	3.16×10^{-6}	0.0793
5	5	−8	6.5	2.5	−7	3.16×10^{-6}	0.0797
6	−3	−2	8.5	12	4	3.16×10^{-6}	0.0793
7	10	−9	11.5	12	−2	3.16×10^{-6}	0.0795
8	11	−5	12.5	12	−1	3.16×10^{-6}	0.0797
9	0.5	3	8	12	−6	3.16×10^{-6}	0.0778
10	6	−10	7.5	8.5	−5	3.16×10^{-6}	0.0792

The corresponding cost denotes the lowest value of the cost function obtained at $N_{generation} = 250$.

Table 4. Evolution of $T_{\equiv S-OH}$ Value Over 250 Generations for 10 Replicated Runs

Run #	$T_{\equiv S-OH}$ (M) $N_{generation} = 1 \rightarrow N_{generation} = 250$				
1	3.16×10^{-3}	1.00×10^{-6}	1.00×10^{-5}	3.16×10^{-4}	**3.16×10^{-6}**
2	1.00×10^{-6}	**3.16×10^{-6}**			
3	3.16×10^{-2}	3.16×10^{-4}	1.00×10^{-2}	**3.16×10^{-6}**	
4	3.16×10^{-3}	3.16×10^{-6}	1.00×10^{-6}	**3.16×10^{-6}**	
5	1.00×10^{-2}	1.00×10^{-3}	**3.16×10^{-6}**		
6	**3.16×10^{-6}**				
7	3.16×10^{-4}	1.00×10^{-2}	1.00×10^{-6}	**3.16×10^{-6}**	
8	1.00×10^{-3}	3.16×10^{-3}	1.00×10^{-5}	1.00×10^{-6}	**3.16×10^{-6}**
9	1.00×10^{-5}	**3.16×10^{-6}**			
10	1.00×10^{-5}	3.16×10^{-6}	1.00×10^{-6}	**3.16×10^{-5}**	

Bold values represent optimized parameter at $N_{generation} = 250$.

differences are more pronounced for small $N_{generation}$ and tend to disappear for $N_{generation} > 90$. The corresponding simulations of the TBT breakthrough curve show that the experimental data are well reproduced (Figure 1b), with quasi-superimposed 10 simulated curves. As demonstrated in Figure 1, GAs are capable of already finding a close approximation to the problem solution with a small number of function evaluations. This initial phase feature is extremely important in reactive transport models where the computation speed is crucial. This GA feature has also been reported in other studies.[39,40]

The optimized values of the TBT sorption parameters for the 10 runs are given in Table 3. Note that $T_{\equiv S-OH}$ converges always to the same value of 3.16×10^{-6} M whereas the other five equilibrium constants log (K) vary from one run to another. One might argue that the GA did not disturb the $T_{\equiv S-OH}$ parameter so that its value remained the same through all the runs. Such a possibility is refuted because we checked out the evolution of the $T_{\equiv S-OH}$ parameter across the generations for the 10 runs (Table 4), and found that $T_{\equiv S-OH}$ generally took several values before converging to 3.16×10^{-6} M (except for run No. 6). The optimized value of $T_{\equiv S-OH}$ is in the same order of that of Aggarwal and Carrayrou,[13] who found $T_{\equiv S-OH}$ values around 6.5×10^{-6} M. Apart from $T_{\equiv S-OH}$, the ensemble of the optimized parameters shows wide variations from one run to another and leads finally to roughly the same cost. This is a typical characteristic of parameter spaces with multiple local minima. Therefore, the use of GAs (as a global method) is fully justified in such a context.

Values of equilibrium constants for TBT sorption are scarce in literature (Table 5). By comparing literature values to our optimization results (Table 3), we see that the optimized log (K) values of this study are in the range of literature values, except for $\equiv$S—OTBT and $\equiv$S—OHTBT$^+$, where we do not get negative values as in Weidenhaupt et al.[30] Meanwhile, we should note that the values given by Weidenhaupt et al.[30] are obtained using pure amorphous silica and the constant capacitance model, whereas our values are obtained using natural quartz sand and the DLM.

Cd test case. To discover the parameter space of the Cd test case, 10 GA runs were replicated (Figure 2). The ensemble evolution of the cost as a function of the number of generations shows that the cost decrease for low $N_{generation}$ values is followed by a slighter one for high $N_{generation}$ values (Figure 2a). Meanwhile, the differences between the 10 runs are much more pronounced in the Cd than in the TBT test case (Figure 1a). Even if the amplitude of these differences gets smaller as $N_{generation}$ increases, it does not tend to vanish before $N_{generation} = 240$. The differences in cost evolution (Figure 2a) are reflected in the corresponding simulations of the Cd breakthrough curve, where we can see little discrepancies among the 10 GA runs (Figure 2b). Nevertheless, the over all simulation of Cd data is quite satisfactory.

The optimized Cd sorption parameters for the 10 runs are given in Table 6. All optimized parameters varied from one run to another, and none of them converged always to a same value (as was observed for $T_{\equiv S_c-OH}$ in the TBT test case). For runs #4 and #10, the same final cost was obtained for two different sets of optimized parameters. This shows that the Cd parameters space is complex and that the risk of the presence of local minima does exist. Once more, the use of GAs is justified in this kind of situation.

A question now arises about having a parameter (i.e., $T_{\equiv S_c-OH}$) in the TBT test-case that always converges to a same value, whereas this is not the case for Cd. The answer

Table 5. Literature Values of TBT Sorption Parameters [log (K) Values] with the Corresponding Type of Surface Site, the Surface Complexation Model, and the Inverse Method Used in Each Study

Reference	Surface Site	Surface Complexation Model	Inverse Method	log (K) $\equiv$S—OH$_2^+$	$\equiv$S—O$^-$	$\equiv$S—OTBT	$\equiv$S—OHTBT$^+$	$\equiv$S—ONa
Weidenhaupt et al.[30]	Kaolinite, illite, and montmorillonite	Constant capacitance model	–		−6.56	−2.47	−1.92	−5.26
Hoch and Weerasooriya[29]	Kaolinite	Double layer model	FITEQL	4.6	−5.4	−2.5 to 3.3		
Aggarwal and Carrayrou[13]	Natural quartz sand	Diffuse layer model	Monte-Carlo	4	−8	1.37	5.46	−5.3

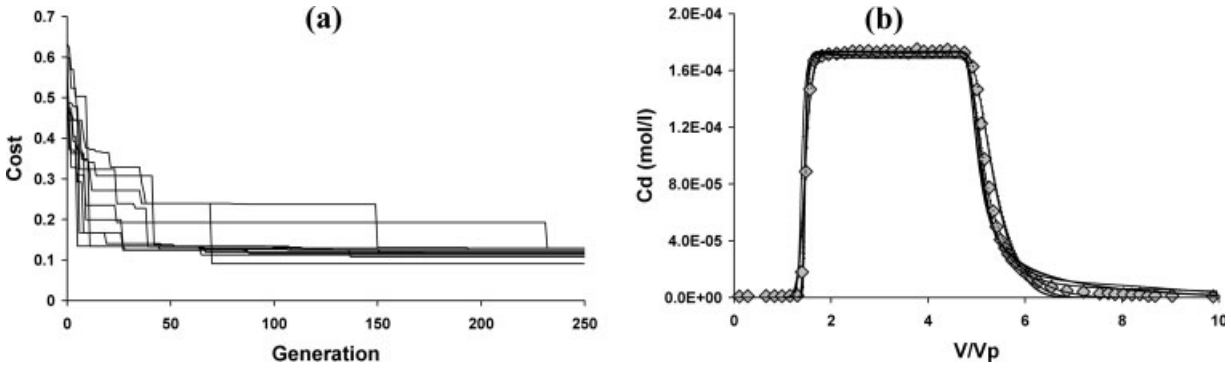

Figure 2. Estimating chemical equilibrium parameters for the Cd reactive transport test case using GA inverse method.

(a) Evolution of the cost function over 250 generations for 10 replicated runs. (b) Experimental breakthrough curve and its simulation with the optimized parameters for 10 replicated runs. ◇ shows experimental data; lines show simulations.

can reside in the different formulation of the chemical problem between the two test cases. In the TBT test case, there is only one initial site concentration to be estimated ($T_{\equiv S_C-OH}$), whereas in the Cd test case, there are two site concentrations to be estimated ($T_{\equiv S_C-OH}$ and $T_{\equiv S_E-Na}$). The two latter site concentrations probably interfere in the reactive transport model so that none of them converges to a stable value.

Cd sorption parameters are more abundant in the literature than those of TBT (Table 7). We should note that the parameter estimation procedure depends on the following conditions: (i) the surface complexation model that is used (DLM, constant capacitance model, double layer model or triple layer model), (ii) the type of surface sites (quartz sand, clay, mixed clay), (iii) experimental conditions (pH, flow rate), and (iv) whether Cd is introduced alone in the porous media or with other ions (such as Cu, Ni, Pb, Co, or Zn). Therefore, we rarely find the same configuration for the ensemble of the previous conditions in separate studies. Therefore, the comparison between parameters values from different studies should be considered with care.

A global comparison between log (K) optimized values of this study (Table 6) and those of other studies (Table 7) shows that, in some runs, our optimization results are in good accordance with other literature values, log ($K_{\equiv S_C-O^-}$) in runs # 3, #4, and #9 compared to those of Choi,[32] Srivastava et al.,[33] and Angove et al.,[37] log ($K_{\equiv S_C-OCdOH}$) in runs #2, #6, and #7 compared with those of Choi,[32] Lackovic et al.,[35] and Angove et al.,[36] log ($K_{\equiv S_E-H}$) in runs #2, #3, and #5 compared with those of Choi,[32] Lackovic et al.,[34] and Angove et al.,[37] and log ($K_{\equiv (S_E)_2-Cd}$) in all runs compared with those of Gu and Evans[31] and Angove et al.[37] However, some of the other runs show a large discrepancy between our results and those of literature, such as log ($K_{\equiv S_C-O^-}$) in runs # 1, #2, and #7, log ($K_{\equiv S_C-OCdOH}$) in runs #1, #3, and #5, and log ($K_{\equiv S_E-H}$) in runs #1, #6, and #7.

Comparison of GA and Monte-Carlo performances

The comparison between the performances of GA and Monte-Carlo methods is based on the variation of the cost as a function of the number of evaluations of the cost function. Because of the stochastic nature of both algorithms, 100 optimization runs were used for each method.

In the TBT test case (Figure 3), the evolution of the minimum cost was evaluated by calculating its mean over 100 runs. The resulting curves show that the GA minimum cost is lower than that of the Monte-Carlo (Figure 3a). Starting from a similar position, the GA minimum cost decreased much more rapidly than that of Monte-Carlo for earlier evaluation numbers. The advantage gained earlier by GA is later conserved. However, for high evaluation numbers, the

Table 6. Optimized Values of Sorption Parameters for the Cd Test Case Using GAs for 10 Replicated Runs

	log (K)						
Run #	$\equiv S_C-O^-$	$\equiv S_C-OCdOH$	$\equiv S_E-H$	$\equiv (S_E)_2-Cd$	$T_{\equiv S_C-OH}$ (M)	$T_{\equiv S_E-Na}$ (M)	Cost
1	0	−7	5	0	1.00×10^{-4}	5.62×10^{-4}	0.078
2	3	−13.5	2	0.5	5.62×10^{-4}	1.78×10^{-4}	0.124
3	−5	−7	−1	0	1.78×10^{-6}	1.78×10^{-4}	0.116
4	−7	−14	−7	−0.5	1.78×10^{-2}	3.16×10^{-4}	0.129
5	−3	−6.5	−3	0.5	1.00×10^{-5}	1.78×10^{-4}	0.113
6	−1	−14	8.5	3	1.00×10^{-3}	1.78×10^{-3}	0.108
7	0	−13.5	7.5	1	5.62×10^{-2}	1.78×10^{-3}	0.090
8	−2	−8.5	4.5	−1.5	3.16×10^{-3}	1.00×10^{-3}	0.085
9	−7	−9.5	4.5	−2	1.00×10^{-2}	5.62×10^{-4}	0.088
10	−5	−7	−5	0.5	5.62×10^{-7}	1.78×10^{-4}	0.129

The corresponding cost denotes the lowest value of the cost function obtained at $N_{generation} = 250$.

Table 7. Literature Values of Cd Sorption Parameters [log (*K*) Values] with the Corresponding Type of Surface Site, the Surface Complexation Model, and the Inverse Method Used in Each Study

Reference	Surface Site	Surface Complexation Model	Inverse Method	log (*K*)			
				$\equiv S_C{-}O^-$	$\equiv S_C{-}OCdOH$	$\equiv S_E{-}H$	$\equiv (S_E)_2{-}Cd$
Gu and Evans[31]	Fithian illite	Constant capacitance model	FITEQL				−0.05 to 1.12
Choi[32]	Smectite and vertisol	Triple layer model	MINTEQA2	−6.65	−11.69	1.04	
Srivastava et al.[33]	Kaolinite	Extended constant capacitance model	GRFIT	−6.16			4.13
Lackovic et al.[34]	Kaolinite and muloorina illite	Extended constant capacitance model	not specified	−7.55		−2.88	3.35
Lackovic et al.[35]	Goethite, illite and kaolinite	Extended constant capacitance model	not specified	−9.4 to −7.55	−12.23	−3.02 to −2.88	3.35 to 5.48
Angove et al.[36]*	Goethite	Constant capacitance model	FITEQL	−9.88	−12.11		
Angove et al.[37]*	Kaolinite	Constant capacitance model	FITEQL	−7.15		−2.88	3.01

*log (*K*) values correspond to a temperature of 25°C.

Monte-Carlo minimum cost curve became more and more close to that of GA. Such behavior is expected because for high evaluation numbers, the stochastic features of both methods tend to become similar, whereas the "intelligent" search of GAs has a net advantage over Monte-Carlo methods for earlier evaluation numbers. Such an advantage is crucial when the cost function is highly time-consuming and when a good solution should be reached within a small number of evaluations.

Concerning the Cd test case, the decrease of the minimum cost curve (for both GA and Monte-Carlo methods) is smoother than for the TBT test case (Figure 3b). We could expect such a result based on the comparison made in the previous subsection between Figures 1a and 2a. As in the TBT test case, the GA minimum cost (for Cd) is always lower than that of the Monte-Carlo (Figure 3b). The net advantage of GA, which was observed from the start of evaluations for TBT (Figure 3a), is somehow delayed in the case of Cd; it becomes pronounced after 60 evaluations of the cost function (Figure 3b). This delay is probably related to the different characteristics of the parameters space for the two test cases. Meanwhile, we would expect that, for high evaluation numbers, the GA advantage (for Cd) will decrease, consequently bringing the GA and Monte-Carlo minimum cost curves much closer. The Cd minimum cost curves would reproduce the behavior of TBT, but with some deformations with respect to the evaluation number (*x*-axis) and the minimum cost (*y*-axis).

Our comparison results are in accordance with other studies. In a recent article concerning slope stability analysis, Sengupta and Upadhyay[41] found that GAs were computationally superior to the Monte-Carlo method. The result of their comparison between GA and Monte-Carlo shows a behavior similar to Figure 3a. In fact, the advantage of GAs is due to their capability of combining the advantages of a randomized approach, such as the Monte Carlo (escape from local minimum), with those of a systematic approach (search for local minimum).

Over 100 runs, we evaluated the algorithm performance by the number of times each inverse method led to the lowest cost for 200 evaluations (Figure 4). In the example of TBT, the GA performance was more than twice that of the Monte-Carlo (Figure 4a), while for the Cd test case, the GA performance was about 2.5 that of the Monte-Carlo (Figure 4b). As aforementioned, we could expect that the gap between the two methods would decrease for higher evaluation numbers.

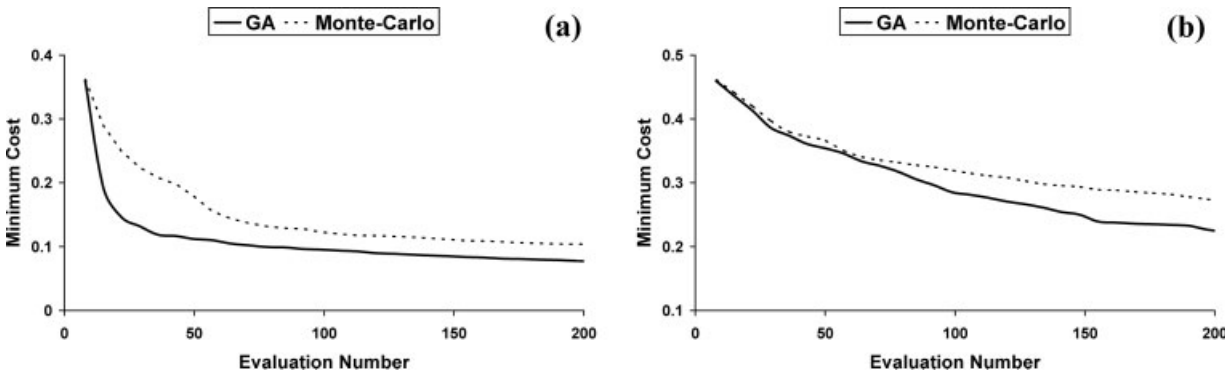

Figure 3. Minimum cost evolution as a function of the number of evaluations of the cost function.

The plotted curves represent the mean cost over 100 replicated runs. (a) TBT test case. (b) Cd test case.

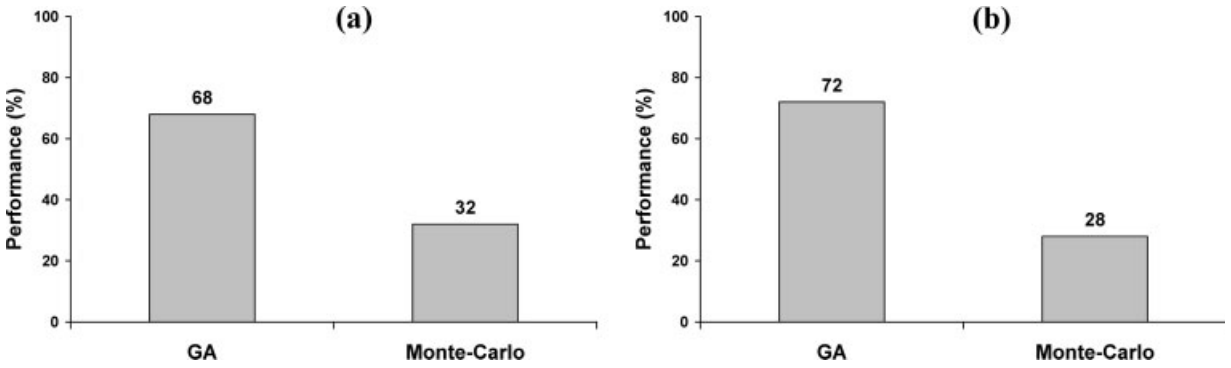

Figure 4. Comparing GA and Monte-Carlo performances over 100 replicated runs.

Performance is evaluated by the number of times over 100 runs each method led to the lowest cost for 200 evaluations of the cost function. (a) TBT test case. (b) Cd test case.

Conclusion

In this article, GAs were used in a first attempt to estimate the chemical equilibrium parameters of a reactive transport model. The transport of Cd and TBT in column experiments was taken as a test case and the optimization concerned the sorption parameters of both compounds onto cristobalite and natural quartz sand, respectively. The GA method is capable of minimizing the difference between experimental and modeled breakthrough curves for both of the Cd and TBT test cases. For several repeated runs, quite satisfactory simulated curves were obtained with a very limited number of evaluations of the cost function (only one per 10^5 of the parameters space). Over the different runs, similar cost values were obtained for varying sets of optimized parameters, which reflects a parameters space with a complex structure (local minima). The use of a global method like GA was thus fully justified in this context. In our study, the comparison between GA and another global method (Monte-Carlo) showed that the GA performance is more than double the Monte-Carlo performance for the two test cases. Especially for a small number of evaluations of the cost function, GA demonstrated a net advantage over the Monte-Carlo approach. The consequences of this comparison can be crucial in predictive models having a highly time-consuming cost function and where an acceptable solution of the problem is recommended for very limited number of evaluations of the cost function. This study shows that the use of GA to estimate the parameters of reactive transport models is promising.

Acknowledgements

This work was supported by the "Agence Nationale de la Recherche": (French national Research Agency) on the "VulNaR" project.

Literature Cited

1. van der Lee J, De Windt L. Present state and future directions of modelling of geochemistry in hydrogeological systems. *J Contam Hydrol*. 2001;47:265–282.
2. MacQuarrie KTB, Ulrich Mayer K. Reactive transport modelling in fractured rock: a state-of-the-science review. *Earth-Sci Rev*. 2005;72:189–227.
3. Fahs M, Carrayrou J, Younes A, Ackerer P. On the efficiency of the direct substitution approach for reactive transport problems in porous media. *Water Air Soil Pollut*. 2008;193:299–308.
4. Christakis N, Wang J, Patel MK, Bradley MSA, Leaper MC, Cross M. Aggregation and caking process of granular materials: continuum model and numerical simulation with application to sugar. *Adv Powder Technol*. 2006;17:543–565.
5. Wang J, Christakis N, Patel MK, Cross M. A numerical model of coupled heat and moisture transfer with phase change in granular material during varying environmental conditions. *Numer Heat Transfer A*. 2004;45:751–776.
6. Vig K, Megharaj M, Sethunathan N, Naidu R. Bioavailability and toxicity of cadmium to microorganisms and their activities in soil: a review. *Adv Environ Res*. 2003;8:121–135.
7. Antizar-Ladislao B. Environmental levels, toxicity and human exposure to tributyltin (TBT)-contaminated marine environment. A review. *Environ Int*. 2008;34:292–308.
8. Davis JA, James RO, Leckie JO. Surface ionization and complexation at the oxide/water interface I. Computation of electrical double layer properties in simple electrolytes. *J Colloid Interface Sci*. 1978;63:480–499.
9. Westall JC. *FITEQL ver. 2.1*. Corvallis, Department of Chemistry, Oregon State University, Corvallis, OR. 1982.
10. Allison JD, Brown DS, Novo-Gradac KJ. *MINTEQA2/PRODEFA2. A Geochemical Assessment Model for Environmental Systems: Version 3.0 User's Manual*. Environmental Research Laboratory, Office of Research and Development, USEPA, Athens, CA. 1990.
11. Ludwig C. *GRFIT: A Program, for Solving Speciation Problems, Evaluation of Equilibrium Constants, Concentrations and Their Physical Parameters*. Switzerland: The University of Berne, 1992.
12. Toride N, Leij FJ, Genuchten MT. *The CXTFIT Code for Estimating Transport Parameters from Laboratory or Field Tracer Experiments (Ver 2.1)*. Riverside, CA: US Salinity Laboratory, Agricultural Research Service, US Department of Agriculture, 1995:140.
13. Aggarwal M, Carrayrou J. Parameter estimation for reactive transport by a Monte-Carlo approach. *AIChE J*. 2006;52:2281–2289.
14. Carrayrou J, Mosé R, Behra P. New efficient algorithm for solving thermodynamic chemistry. *AIChE J*. 2002;48:894–904.
15. Brassard P, Bodurtha P. A feasible set for chemical speciation problems. *Computers Geosci*. 2000;26:277–291.
16. Holland JH. *Adaptation in Natural and Artificial Systems*. Ann Arbor: University of Michigan Press, 1975.
17. Goldberg DE. *Genetic Algorithms in Search, Optimization, and Machine Learning*. New York: Addison-Wesley, 1989.
18. Majdalani S, Angulo-Jaramillo R, Di Pietro L. Estimating preferential water flow parameters using a binary genetic algorithm inverse method. *Environ Model Software*. 2008;23:950–956.
19. Sarkar D, Rohani S, Jutan A. Multiobjective optimization of semibatch reactive crystallization processes. *AIChE J*. 2007;53:1164–1177.
20. Low KH, Sørensen E. Simultaneous optimal configuration, design and operation of batch distillation. *AIChE J*. 2005;51:1700–1713.
21. Hugget A, Sébastian P, Nadeau JP. Global optimization of a dryer by using neural networks and genetic algorithms. *AIChE J*. 1999;45:1227–1238.

22. Goldberg DE. The design of innovation: lessons from genetic algorithms, lessons for the real world. *Technol Forecast Social Change*. 2000;64:7–12.
23. Matott LS, Rabideau AJ. Calibration of subsurface batch and reactive-transport models involving complex biogeochemical processes. *Adv Water Resour*. 2008;31:269–286.
24. Massoudieh A, Mathew A, Ginn TR. Column and batch reactive transport experiment parameter estimation using a genetic algorithm. *Computers Geosci*. 2008;34:24–34.
25. Bürgisser CS. *Transportverhalten von Nicht-Linear Sorbierenden Stoffen in Chromatographischen Säulen am Beispiel der Adsorption an Cristobalit, PhD Thesis*. Zurich: Swiss Federal Institute of Technology, 1994.
26. Bueno M, Astruc A, Astruc M, Behra P. Dynamic sorptive behaviour of tributyltin on quartz sand at low concentration levels: effect of pH, flow rate, and monovalent cations. *Environ Sci Technol*. 1998;32:3919–3925.
27. Yeh GT, Tripathi VS. A critical evaluation of recent developments in hydrogeochemical transport models of reactive multichemical components. *Water Resour Res*. 1989;25:93–108.
28. Haupt RL, Haupt SE. *Practical Genetic Algorithms*, 2nd edition. New York: Wiley, 2004.
29. Hoch M, Weerasooriya R. Modeling interactions at the tributyltin-kaolinite interface. *Chemosphere*. 2005;59:743–752.
30. Weidenhaupt A, Arnold C, Müller SR, Haderlein SB, Schwarzenbach RP. Sorption of organotin biocides to mineral surfaces. *Environ Sci Technol*. 1997;31:2603–2609.
31. Gu X, Evans LJ. Modelling the adsorption of Cd(II), Cu(II), Pb(II), and Zn(II) onto fithian illite. *J Colloid Interface Sci*. 2007;307:317–325.
32. Choi J. Geochemical modelling of cadmium sorption to soil as a function of soil properties. *Chemosphere*. 2006;63:1824–1834.
33. Srivastava P, Singh B, Angove M. Competitive adsorption behaviour of heavy metals on kaolinite. *J Colloid Interface Sci*. 2005;290:28–38.
34. Lackovic K, Angove MJ, Wells JD, Johnson BB. Modeling the adsorption of Cd(II) onto kaolinite and muloorina illite in the presence of citric acid. *J Colloid Interface Sci*. 2004;270:86–93.
35. Lackovic K, Wells JD, Johnson BB, Angove MJ. Modeling the adsorption of Cd(II) onto muloorina illite and related clay minerals. *J Colloid Interface Sci*. 2003;257:31–40.
36. Angove MJ, Wells JD, Johnson BB. The influence of temperature on the adsorption of cadmium (II) and cobalt (II) on goethite. *J Colloid Interface Sci*. 1999;211:281–290.
37. Angove MJ, Johnson BB, Wells JD. The influence of temperature on the adsorption of cadmium (II) and cobalt (II) on kaolinite. *J Colloid Interface Sci*. 1998;204:93–103.
38. Deb K, Agrawal S. Understanding interactions among genetic algorithm parameters. In Banzhaf W, Reeves C, editor. *Foundations of Genetic Algorithms 5*. San Francisco, CA: Morgan Kaufmann, 1999:265–286.
39. Rauch W, Harremoës P. On the potential of genetic algorithms in urban drainage modelling. *Urban Water*. 1999;1:79–89.
40. Rauch W, Harremoës P. Genetic algorithms in real-time control applied to minimize transient pollution from urban wastewater systems. *Water Res*. 1999;33:1265–1277.
41. Sengupta A, Upadhyay A. Locating the critical failure surface in a slope stability analysis by genetic algorithm. *Appl Soft Comput J*. 2009;9:387–392.

Manuscript received Aug. 5, 2008, revision received Oct. 28, 2008, and final revision received Dec. 3, 2008.